The Company of **Biologists**

RESEARCH ARTICLE

A Nodal/Eph signalling relay drives the transition from apical constriction to apico-basal shortening in ascidian endoderm invagination

Ulla-Maj Fiuza[1,§], Takefumi Negishi[2,*], Alice Rouan[2,‡], Hitoyoshi Yasuo[2,§] and Patrick Lemaire[1,§]

ABSTRACT

Gastrulation is the first major morphogenetic event during animal embryogenesis. Ascidian gastrulation starts with the invagination of 10 endodermal precursor cells between the 64- and late 112-cell stages. This process occurs in the absence of endodermal cell division and in two steps, driven by myosin-dependent contractions of the acto-myosin network. First, endoderm precursors constrict their apex. Second, they shorten apico-basally, while retaining small apical surfaces, thereby causing invagination. The mechanisms that prevent endoderm cell division, trigger the transition between step 1 and step 2, and drive apico-basal shortening have remained elusive. Here, we demonstrate a conserved role for Nodal and Eph signalling during invagination in two distantly related ascidian species, *Phallusia mammillata* and *Ciona intestinalis*. Specifically, we show that the transition to step 2 is triggered by Nodal relayed by Eph signalling. In addition, our results indicate that Eph signalling lengthens the endodermal cell cycle, independently of Nodal. Finally, we find that both Nodal and Eph signals are dispensable for endoderm fate specification. These results illustrate commonalities as well as differences in the action of Nodal during ascidian and vertebrate gastrulation.

KEY WORDS: Nodal, Ephrin, Gastrulation, Morphogenesis, Cell fate

INTRODUCTION

Epithelial invagination, the buckling of a sheet of cells into a cup-like structure, is a morphogenetic mechanism that drives dramatic tissue shape changes in multiple embryonic contexts including neurulation, optic cup formation and gastrulation. In most metazoans, endoderm invagination is the first event of gastrulation, a key embryonic process during which the embryo body plan is laid out and the main tissue types become specified (Leptin, 2005; Solnica-Krezel and Sepich, 2012). Although the precise coordination of cell fate decisions, cell shape changes, cell divisions and cell movements is crucial to ensure successful embryogenesis, we only have a fragmented understanding of the way these processes are integrated at the transcriptional level (reviewed by Heisenberg and Solnica-Krezel, 2008).

In this study, we explore the mechanisms controlling endoderm invagination in *Phallusia mammillata* and *Ciona intestinalis*, two species of solitary phlebobranch ascidians, a group of marine invertebrate chordates closely related to vertebrates (Delsuc et al., 2006). Although they diverged more than 200 million years ago (Delsuc et al., 2018), these two species develop in a remarkably similar manner, with small cell numbers and shared stereotypic invariant cell lineages. Exactly 10 endoderm precursor cells actively drive endoderm invagination at the onset of gastrulation. This precise cellular framework is ideal to characterise the chain of molecular events occurring in each precursor, which collectively drive invagination (reviewed by Lemaire, 2011).

Previous work has established that invagination is a two-step process, conserved between *P. mammillata* and *C. intestinalis* (Sherrard et al., 2010; Fig. 1A). During step 1, endoderm cells apically constrict, leading to a flattening of the vegetal side of the embryo. During step 2, endoderm invagination proper takes place when endoderm cells shorten along their apico-basal axis while maintaining small apical surfaces. Both steps are controlled by Myosin II, via the phosphorylation of its regulatory light chain either at Ser19 (1P-Myosin) or at Ser19 and Thr18 (2P-Myosin) (Sherrard et al., 2010). During step 1, endoderm apical constriction is mediated by the apical accumulation of 1P-Myosin in response to Rho-associated kinase (ROCK). During step 2, sub-apical 2P-Myosin accumulation ensures that apical surfaces remain small, whereas baso-lateral 1P-Myosin drives apico-basal shortening. Sub-apical 2P-Myosin accumulation is ROCK-dependent, but neither ROCK, RhoA, Rac nor Cdc42 are required for the baso-lateral accumulation of 1P-Myosin. Finally, the two steps operate relatively independent of each other, as inhibition of step 1 does not prevent step 2 apico-basal shortening (Sherrard et al., 2010).

These previous studies have established ascidian endoderm invagination as a powerful model to dissect the molecular control mechanisms of a seemingly simple morphogenetic process. Yet, they left several key questions unanswered. First, they neither identified the apical activators of ROCK during step 1 and 2, nor the pathway(s) controlling the baso-lateral accumulation of 1P-Myosin during step 2. Second, what triggers the transition between the two steps is unknown. Third, the mechanisms ensuring that endoderm cell division is delayed until step 2 is completed remain ill-defined. Finally, the extent of coupling between the acquisition of the endodermal fate and the control of cell shape is also unknown. In this study, we addressed several of these issues, and identified Nodal and Ephrin receptor (Eph) signalling as key regulators of the transition between the two steps and, for the latter pathway, in the lengthening of the endodermal cell cycle. Furthermore, our results reveal that morphogenetic control can be partially uncoupled from the control of endoderm fate specification.

[1]CRBM, University of Montpellier, CNRS, F-34090 Montpellier, France. [2]Laboratoire de Biologie du Développement de Villefranche-sur-Mer, Sorbonne Universités, CNRS, F-06230 Villefranche-sur-Mer, France.
*Present address: Multicellular Organization Laboratory, National Institute of Genetics, 1111 Yata, Mishima, Shizuoka 411-8540, Japan. ‡Present address: Institute of Research on Cancer and Aging of Nice, Université de la Côte d'Azur, CNRS, F-06000 Nice, France.

§Authors for correspondence (patrick.lemaire@crbm.cnrs.fr; yasuo@obs-vlfr.fr; ulla.maj.fiuza@embl.de)

U.-M.F., 0000-0002-8691-0325; T.N., 0000-0002-0306-9578; H.Y., 0000-0002-0817-3796; P.L., 0000-0003-4925-2009
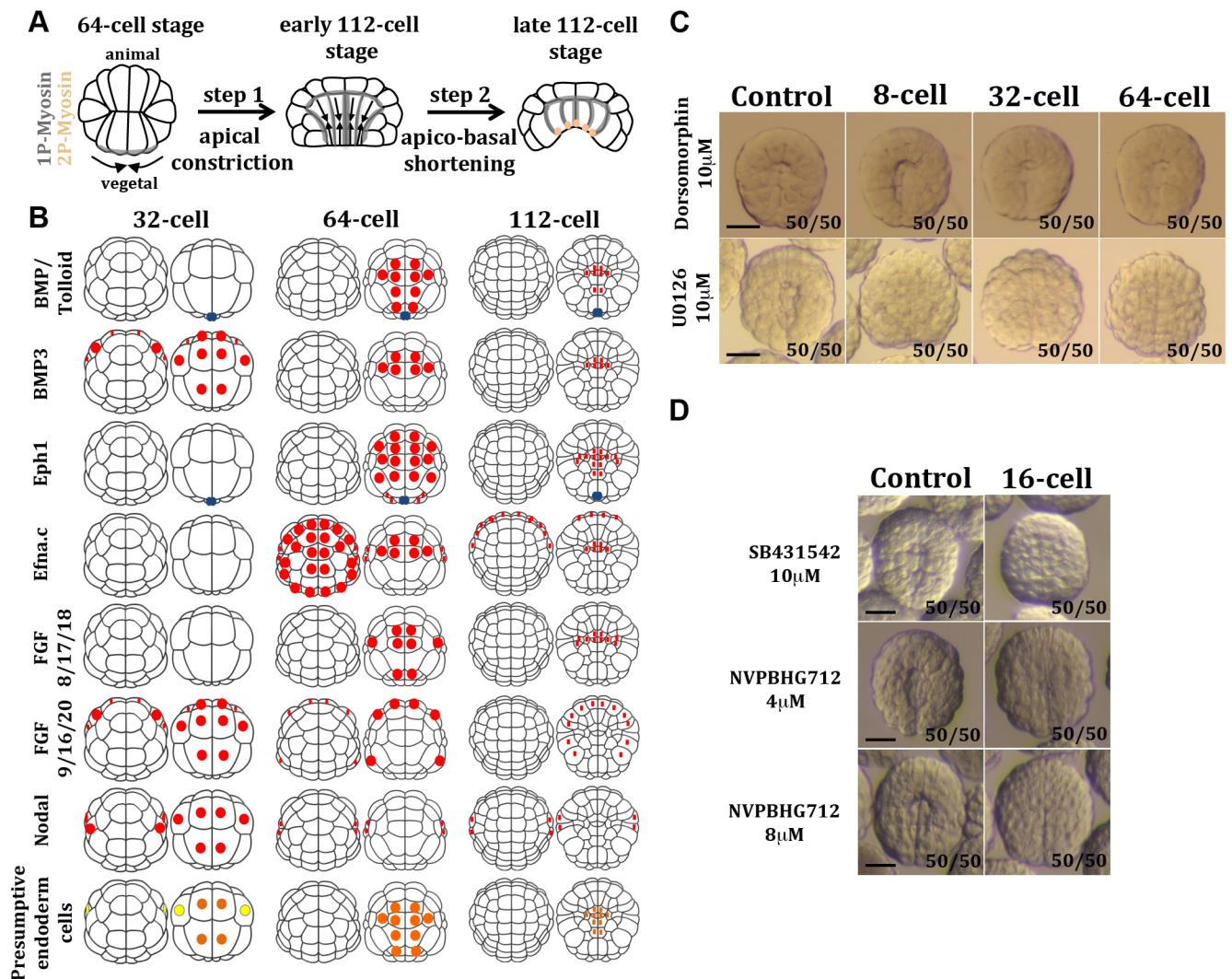
DEVELOPMENT

Fig. 1. Nodal and Eph signalling regulate endoderm invagination in *P. mammillata*. (A) Schematic of endodermal invagination in ascidian early embryos. (B) Schematics of the animal (left panels for each stage) and vegetal (right panels) hemispheres of *Ciona* embryos showing the expression pattern of developmental signalling ligands with predominantly vegetal expression in pre-gastrula stages (Imai et al., 2004; Yasuo and Hudson, 2007; Hudson and Yasuo, 2005). Zygotic expression is shown in red, maternal mRNA in blue, fate-restricted primary endoderm precursors are in orange and pluripotent precursors giving rise to some primary endoderm are in yellow. (C) Late 112-cell stage *P. mammillata* embryos treated with pharmacological inhibitors of BMP (Dorsomorphin at 10 μM) and FGF (U0126 at 10 μM; MEK inhibitor) signalling. Treatment was initiated at the 8-, 32- and 64-cell stages as indicated. (D) Late 112-stage *P. mammillata* embryos treated with pharmacological inhibitors of Nodal (SB431542; Alk4/5/7 inhibitor) and Eph (NVPBHG712; Eph kinase inhibitor) receptors from the 16-cell stage. In C and D the phenotype quantification is shown as the number of embryos exhibiting a phenotype/total number of embryos analysed. Scale bars: 50 μm.

RESULTS

Nodal and Eph signals are required for endoderm invagination independently of mesendoderm specification

In *Drosophila* (Costa et al., 1994), *Caenorhabditis elegans* (Lee et al., 2006) or vertebrates (Heisenberg and Solnica-Krezel, 2008), cell behaviours during gastrulation are controlled by cell-cell communication. Several pathways have been implicated in the control of vertebrate gastrulation movements, including Wnt/PCP (Heisenberg and Solnica-Krezel, 2008), Nodal (Luxardi et al., 2010), FGF (Ciruna and Rossant, 2001) and Bmp (von der Hardt et al., 2007). In ascidians, the non-canonical Wnt/PCP pathway is unlikely to control invagination as mutation of *Prickle*, a core component transcriptionally activated from the 64-cell stage (Brozovic et al., 2018), does not affect *Ciona* gastrulation (Jiang et al., 2005). Inhibition of the canonical Wnt/β-catenin pathway prevents ascidian gastrulation, but this phenotype is the indirect consequence from an early misspecification of the vegetal hemisphere (Imai et al., 2000; Hudson et al., 2013).

Previous work in *Ciona*, summarised in Fig. 1B, has revealed that ligands for the FGF, Bmp, Nodal and Eph developmental signalling pathways are transcriptionally active in pre-gastrula endoderm precursors (Hudson et al., 2003; Imai et al., 2004, 2006; Shi and Levine, 2008; Yasuo and Hudson, 2007) (Fig. 1B, Fig. S1) and may therefore be candidate regulators of endoderm invagination.

Two FGFs are expressed in endoderm precursors before the onset of gastrulation. FGF9/16/20 is expressed transiently in most vegetal cells at the 32-cell stage, whereas FGF8/17/18 is expressed in some endoderm precursors at the 64- and 112-cell stages. Previous work has shown that *Ciona* gastrulation was affected by the inhibition of FGF/ERK signalling (Hudson et al., 2003). Consistently, we found that inhibition of the ERK-kinase MEK, with 10 μM U0126 from the 8- to the 64-cell stages, prevented invagination (Fig. 1C). This phenotype was not due to a failure of step 2. In the absence of MEK activity, endoderm precursors prematurely divided along their apico-basal axis (Guignard et al. 2020), consistent with their

previously documented fate switch to non-invaginating trunk lateral cells (Shi and Levine, 2008).

Bmp3 is expressed in most vegetal cells at the 32-cell stage and becomes restricted to the anterior endodermal cells at the 64- and 112-cell stages. Inhibition of Bmp signalling by overexpression of *Chordin* or *Noggin* in the distantly related ascidian *Halocynthia roretzi* had no major effect on gastrulation, but prevented the formation of sensory head pigment cells (Darras and Nishida, 2001). Consistently, treatment of *Phallusia* embryos from the 8-, 32- or 64-cell stages with 10-12.5 µM of the Bmp receptor inhibitor Dorsomorphin (Yu et al., 2008) prevented the formation of pigmented cells. These treatments did not affect invagination, except for a minority of embryos treated at the 8-cell stage with 12.5 µM Dorsomorphin, in which endoderm invagination was delayed, possibly reflecting a general slowdown of development as the embryos eventually recovered and formed larvae (Fig. 1C, Fig. S2).

Nodal is transiently expressed throughout the vegetal hemisphere at the 32-cell stage, and its expression pattern is perfectly conserved between *Ciona* and *Phallusia* (Madgwick et al., 2019; Fig. S3A). Inhibition of the Nodal pathway was previously shown to impair gastrulation movements in *C. intestinalis* (Hudson and Yasuo, 2005; Hudson et al., 2007), but these studies did not investigate whether this was because of an interference with endoderm invagination or with later processes. Inhibition of Nodal signalling in *P. mammillata* embryos by treatment from the 16-cell stage with SB431542 (5-10 µM), a selective pharmacological inhibitor of the Nodal receptor ALK4/5/7, blocked invagination (Fig. 1D). Consistent with

a specific effect of the inhibitor on the Nodal receptor, the same phenotype was observed following the overexpression of a dominant negative form of the Nodal receptor ALK4/5/7 (Ciinte.tAlk4/5/7; Hudson and Yasuo, 2005) in *Phallusia* (Fig. S4A). This early gastrula invagination phenotype did not reflect a simple delay in endoderm invagination, as no invagination was detected in *Phallusia* late gastrulae treated with SB431542 from the 16-cell stage (Fig. S4B). Interestingly, although in vertebrates Nodal controls both morphogenesis and mesendoderm fate specification (reviewed by Kiecker et al., 2016), inhibition of this signalling pathway in ascidian vegetal territories did not alter the specification of germ layers: expression levels of both early (Fig. 2A) and late (Fig. 2B) vegetal endodermal and mesodermal markers were not reduced by Nodal inhibition. Inhibition of Rock, the main driver of the first step of invagination, also did not affect endoderm and mesoderm specification (Fig. 2B), suggestive of a broad uncoupling of morphogenetic and fate specification mechanisms during early ascidian embryogenesis.

Finally, the gene encoding the ephrinA ligand Efna.c is expressed in the A-line endoderm from the 64-cell stage. The Eph1 receptor is initially expressed in most *Ciona* vegetal cells at the 64-cell stage and becomes progressively restricted to endodermal and TLC progenitors at the 112-cell stage. In *Phallusia*, *Eph1* starts to be expressed at the 64-cell stage and is restricted from this stage onwards to the endoderm and TLC lineages (Fig. S3B). The small molecule inhibitor NVPBHG712 has been described as a selective inhibitor of EphB kinases in mammalian systems (Martiny-Baron et al., 2010) and has been shown to inhibit the single Eph receptor of the sea urchin
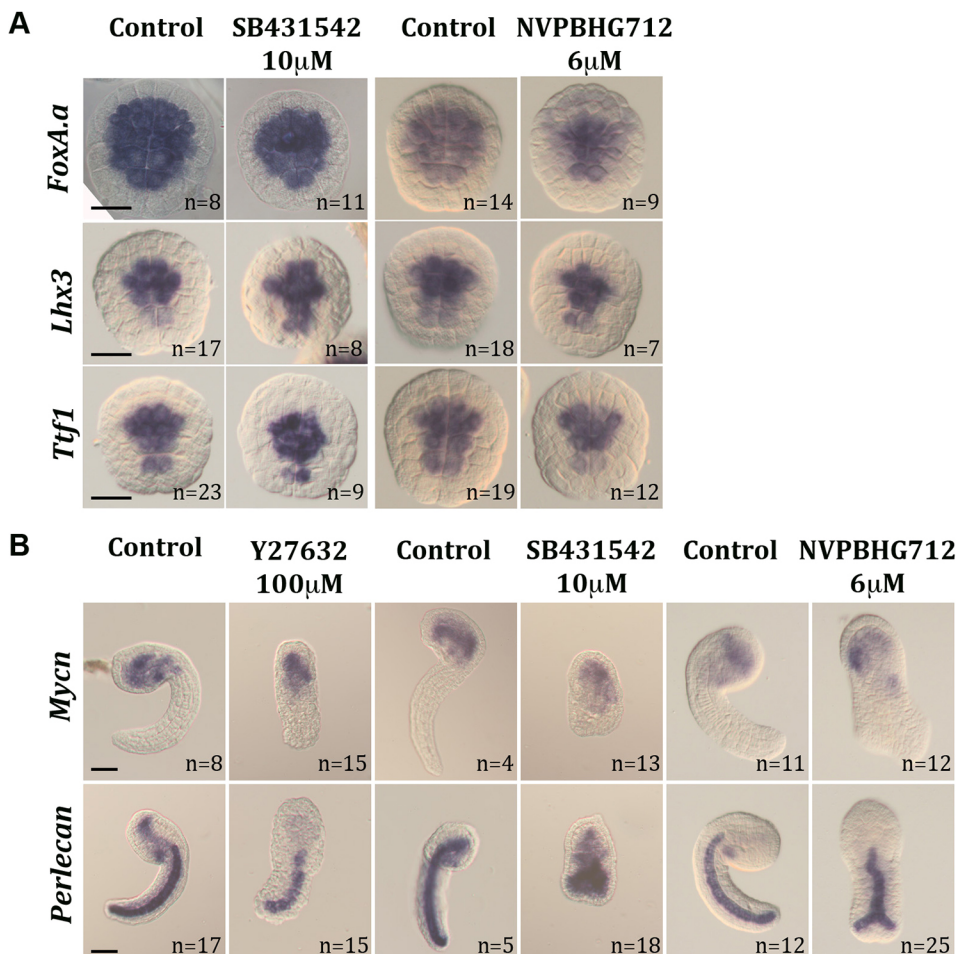

Fig. 2. Nodal and Eph signalling are not necessary for vegetal mesendodermal cell fate specification. (A) WMISH of *Phallusia* embryos at the early 112-cell stage using probes for *FoxA.a* (early mesendoderm marker), *Lhx3* and *Ttf1*, three transcription factors involved in endoderm cell fate specification. Nodal signalling was inhibited by treating the embryos with 10 µM SB431542 from the 16-cell stage. Eph-mediated signalling was inhibited with 6 µM NVPBHG712 from the 8-cell stage. (B) WMISH of *Phallusia* embryos at the mid tailbud II stage, using probes for *Mycn* (late endoderm marker) and *Perlecan* (late notochord marker) under control untreated conditions or following blockade of step 1 of endoderm invagination (100 µM of the ROCK inhibitor Y27632 from 64-cell stage) or of step 2 of endoderm invagination by inhibiting Nodal signalling (10 µM SB431542 from the 16-cell stage) or Eph signalling (6 µM NVPBHG712 from the 8-cell stage). The inhibitors were dissolved in DMSO (SB431542, NVPBHG712) or H$_2$O (Y27632) and control embryos were cultured in the same solvent concentration as the inhibitor-treated embryos. Scale bars: 50 µm.

Strongylocentrotus purpuratus (Krupke and Burke, 2014). Eph receptors having undergone independent gene duplication events in ascidians and vertebrates, each of the ascidian Eph receptors (the *Ciona* and *Phallusia* genomes harbour 6 and 5 Eph receptors, respectively) is orthologous to both EphA and EphB vertebrate receptors. To test whether NVPBHG712 could also inhibit ascidian Eph receptors, we treated 16-cell stage *Ciona* embryos with 4-8 µM of this inhibitor and verified that this treatment phenocopied the known effect of Eph3 signalling inhibition in early neural (Ohta and Satou, 2013) and notochord (Picco et al., 2007) induction (Fig. S5). In addition, this treatment blocked endoderm invagination in both *Ciona* and *Phallusia* (Fig. 1D, Fig. S4F) without preventing early or late vegetal endoderm or mesoderm marker gene expression in *Phallusia* (Fig. 2).

We conclude from this section that Nodal and Eph signalling are required for endoderm invagination at the onset of gastrulation, but not germ layer fate specification in both *Ciona* and *Phallusia*. FGF signalling is also required for invagination, presumably through its role in endoderm induction. Finally, Bmp signalling inhibition has, at best, a weak effect on invagination. These results argue for a broad uncoupling of morphogenetic and fate specification mechanisms. In the following sections, we further studied the mode of action and epistatic relationships of the Nodal and Eph pathways.

Both Nodal and Eph signalling are required for the transition to step 2

As all 10 endoderm precursors undergo simultaneous and similar shape changes during endoderm invagination (Sherrard et al., 2010), we focused our analyses on the cell shape changes taking place in the A7.1 endoderm precursor. To understand which step of the invagination process was affected by Nodal and Eph signalling inhibition, we compared the height, apical and basal areas of the A7.1 cell (Fig. 3A) in control and in pathway-inhibited embryos.

Nodal receptor inhibition with SB431542 from the 16-cell stage in *Phallusia* embryos did not prevent apical constriction (Fig. 3B). By the late 112-cell stage, however, A7.1 cells were significantly taller in SB431542-treated embryos than in controls. Nodal signalling is thus dispensable for step 1 apical constriction but required for step 2 apico-basal shortening of endodermal precursors. Likewise, inhibition of Eph signalling by NVPBHG712 treatment from the 8-cell stage in *Phallusia* and *Ciona* embryos left step 1 unaffected, while preventing correct apico-basal shortening of endodermal precursors during step 2 (Fig. 3C).

Localised Myosin II contractility is the major driving force of ascidian endoderm invagination and is regulated by the phosphorylation state of its regulatory subunit (Sherrard et al., 2010). In control embryos during step 1 (apical constriction), 1P-Myosin first accumulates in speckles on the apical surface of vegetal cells (control 76-cell embryos in Fig. 4A,B), a signal which subsequently gradually decreases. During step 2 (apico-basal shortening), 1P-Myosin has disappeared from the apical side of endoderm progenitors and is detected on the baso-lateral surfaces of endoderm cells (control E112- and L112-cell embryos in Fig. 4A,B).

Upon Nodal signalling inhibition from 16-cell stage (Fig. 4A, SB431542), the apical 1P-Myosin pattern of step 1 was established normally and appeared reinforced at the 76-cell and early 112-cell stages. 1P-Myosin apical accumulation, however, persisted throughout the 112-cell stage, whereas 1P-Myosin did not accumulate on the baso-lateral sides. Similarly, in Eph-inhibited embryos (Fig. 4B, NVPBHG712), 1P-Myosin accumulated apically during step 1 as in wild-type but retained its apical localisation throughout the 112-cell stage without detectable baso-lateral reinforcement.

We conclude that Eph and Nodal signalling are required for the transition from step 1 to step 2. When either of these pathways is inhibited, step 1 occurs normally up to the early 112-cell stage. During the 112-cell stage, however, endodermal cells retain a step 1 pattern of 1P-Myosin localisation and never transition to step 2.

Nodal signalling sets the level of expression of *Eph1* in vegetal territories

We next explored the relationships between Nodal and Eph signalling during invagination. In both species, *Nodal* is first transiently expressed at the 32-cell stage in most vegetal cells, including the endoderm precursors (Fig. S3, Imai et al., 2004). By the 64-cell stage, its expression becomes restricted to animal b-line ectodermal cells (Fig. S3). SB431542 has been shown to rapidly penetrate cells and abrogate Nodal target gene expression within 40 min (Hudson et al., 2007). Early inhibition of Nodal signalling in *Phallusia* embryos either from the 16-cell stage onwards or for a shorter period between the 16- and 64-cell stages prevented endoderm invagination. Inhibition from the 64-cell stage onwards, however, had no major effect on endoderm invagination (Fig. 5A). Nodal signalling during the 32-cell stage, when Nodal is expressed transiently in most vegetal cells, thus appears to be essential for endoderm invagination. This early requirement for Nodal signalling, more than an hour before the onset of invagination at the early 112-cell stage, suggests that this signalling pathway may indirectly regulate the transition to step 2, via a transcriptional relay.

Because Eph signalling inhibition has a similar phenotype as Nodal inhibition, a component of the Eph pathway may transcriptionally relay the action of Nodal. In both *Ciona* and *Phallusia*, a single ligand, *Efna.c*, and a single receptor, *Eph1*, are expressed in endoderm precursors at the time of endoderm invagination (Madgwick et al., 2019; Fig. S3B). *Efna.c* is expressed in A-line endodermal cells from the 76-cell stage. This expression is not affected by Nodal signalling inhibition (Fig. S3C).

Eph1 is zygotically expressed from the 64-cell stage, ~45 min after the onset of *Nodal* expression in endoderm precursors (Fig. S3, Imai et al., 2004). Vegetal *Eph1* expression, initially very low, increases during endoderm invagination. To test whether Nodal signalling is regulating zygotic *Eph1* expression, *Phallusia* embryos were treated with SB431542 from the 16-cell stage and *Eph1* expression was assessed by whole-mount *in situ* hybridisation (WMISH) (Fig. 5B). Nodal signalling inhibition did not qualitatively change the spatial domain of zygotic *Eph1* expression, indicating the presence of Nodal-independent *Eph1* transcriptional activators in endodermal precursors. Nodal signalling inhibition did, however, markedly reduce the intensity of zygotic *Eph1 in situ* signal (Fig. 5B), compared with the maternal signal in the presumptive germline precursors (Fig. 5B, arrowheads), serving as a reference.

Consistent with an involvement of *Eph1* in endoderm invagination, morpholino-mediated knockdown of this gene in *Ciona* embryos disrupted endoderm apico-basal shortening without causing defects in endoderm apical constriction (Fig. S4D,E). Consistent with data obtained with the NVPBHG712 inhibitor, endoderm and mesoderm marker gene expression was also not affected by Eph1 morpholino injection (Fig. S6). These data confirm the effect of the pharmacological Eph inhibition and indicate that *Eph1* may be a Nodal transcriptional target.

We conclude that Nodal signalling sets the level, but not the spatial pattern, of zygotic expression of *Eph1* in the endoderm. Combined with the similarity of the phenotypes resulting from
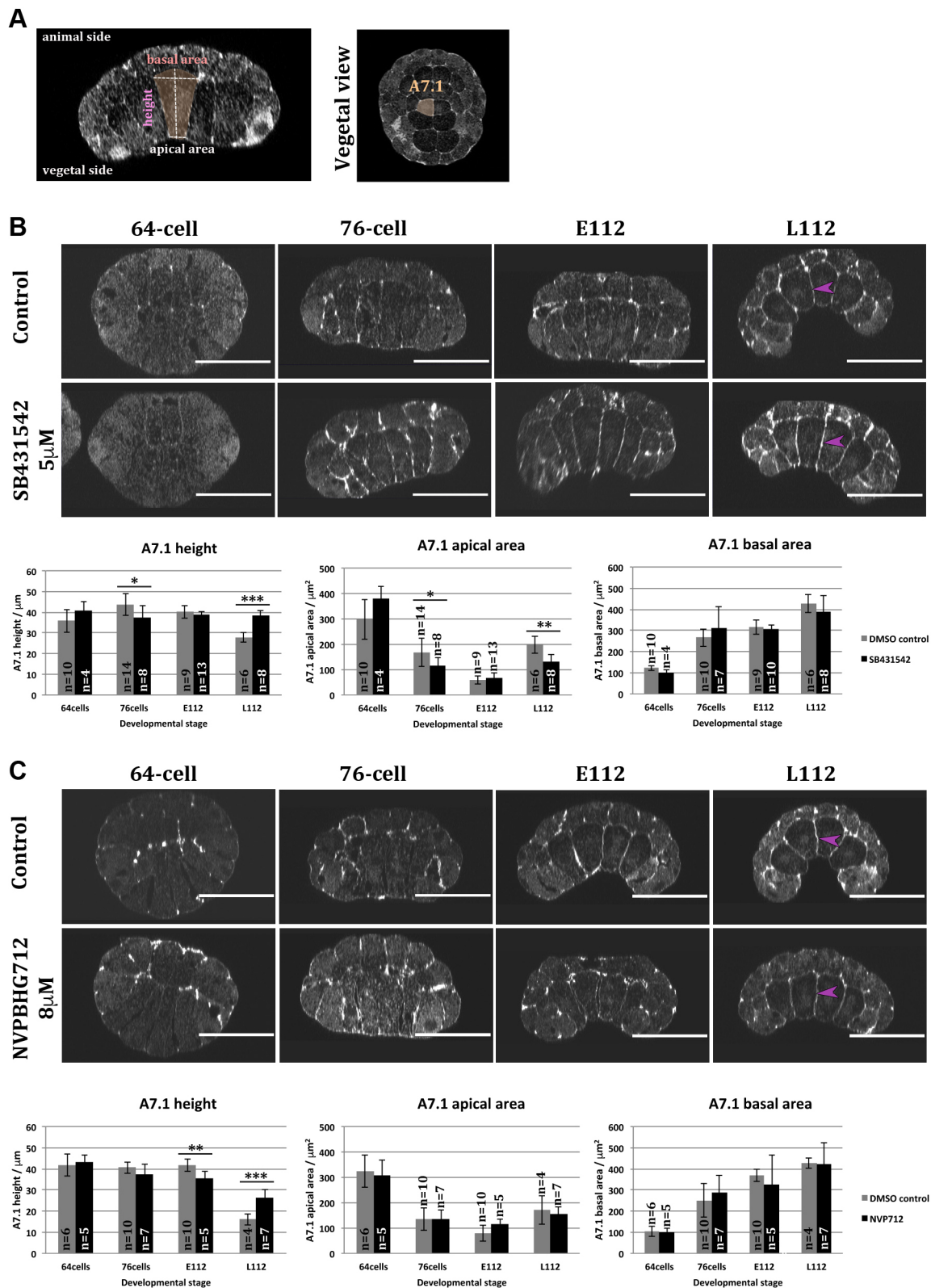
Fig. 3. Nodal or Eph signalling inhibition causes defects in endoderm apico-basal shortening. (A) Schematic of the morphological measurements made in the frontal view and identification of A7.1 cell in a vegetal view of an early 112-cell stage *Phallusia* embryo. (B,C) Effects of Nodal (B) and Eph (C) signal inhibition on endoderm invagination. The experimental embryos were treated with 5 μM SB431542 (B) from the 16-cell stage or with 8 μM NVPBHG712 (C) from the 8-cell stage as indicated. Each photograph shows a frontal optical section of *Phallusia* embryos stained with fluorescent phalloidin to reveal cortical actin at the 64-, 76-, early 112-cell (E112) and late 112-cell (L112) stages. Animal side is up and vegetal side is down. Arrowheads highlight the difference in endoderm cell height between control and pharmacological perturbed embryos at L112. Bar graphs show quantification of the left A7.1 cell height, apical area and basal area of imaged embryos. *P<0.05, **P<0.01, ***P<0.001 (unpaired, two-tailed *t*-test). Error bars indicate s.d. Scale bars: 50 μm.
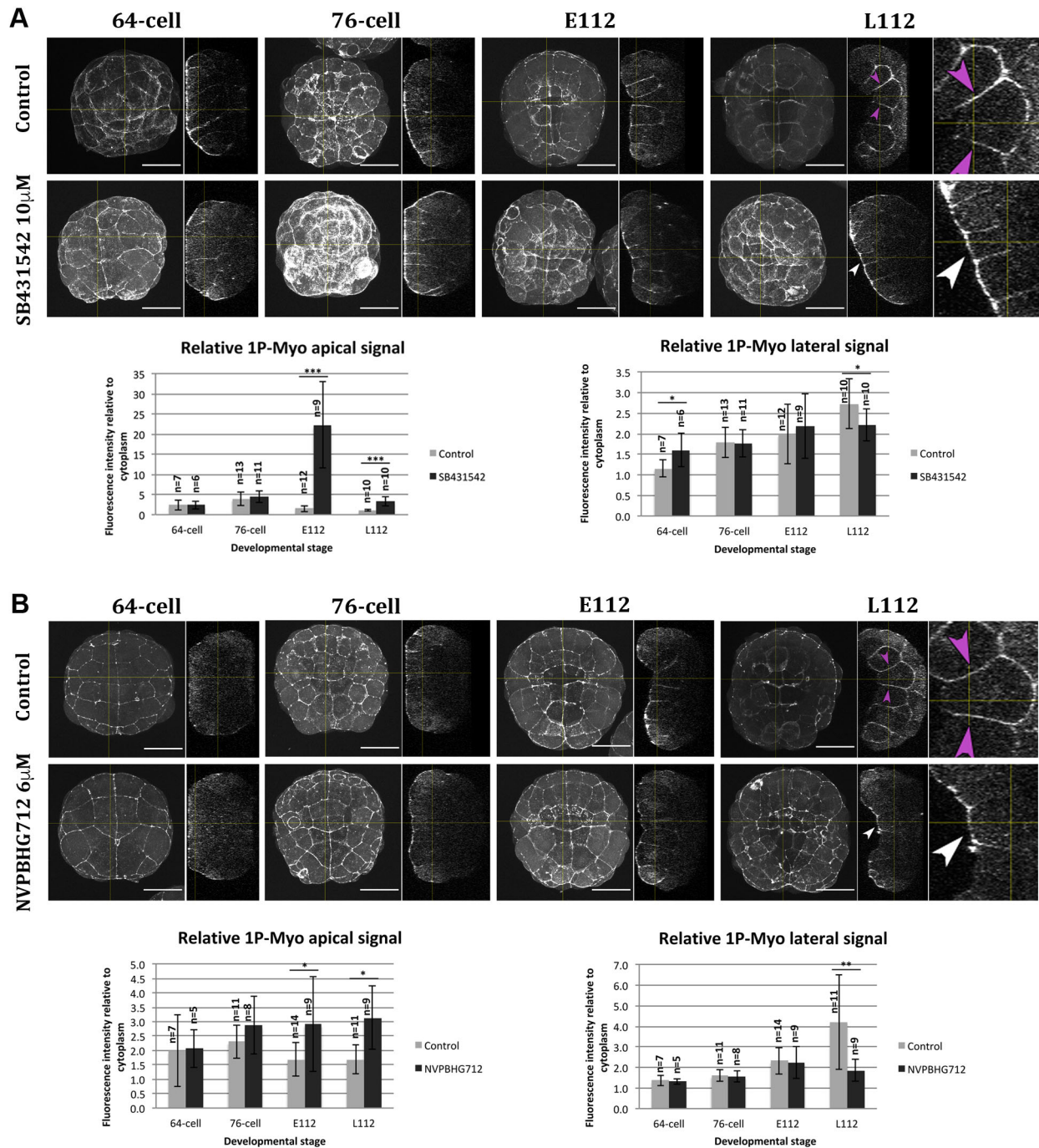
Fig. 4. Nodal and Eph signalling regulate the transition between apical constriction and apico-basal shortening during endoderm invagination by modulating the pattern of 1P-Myosin. (A) 1P-Myosin immunostainings of fixed *Phallusia* embryos treated with either DMSO (Control: top panels) or 10 μM SB431542 (middle panels) from 16-cell stage. (B) 1P-Myosin immunostainings of control *Phallusia* embryos (Control: top panels) or embryos treated with 6 μM NVPBHG712 (middle panels) from 16-cell stage. Embryos are shown both in vegetal pole view (maximal projection) and in sagittal optical section (along the vertical yellow line in the vegetal pole view image) for each of the 64-cell, 76-cell, early 112-cell (E112) and late 112-cell (L112) stages. In addition, a higher magnification of a portion of a sagittal section is shown at the late 112-cell stage. On all sagittal sections, the vegetal side of the embryo is to the left and the animal side to the right. Magenta arrowheads highlight lateral 1P-Myosin signals of endoderm precursors; white arrowheads highlight apical 1P-Myosin signals at L122 stage. Bar graphs show relative intensities (cortical/cytoplasmic) of 1P-Myosin fluorescence signals in apical and lateral cortical domains of A7.1 cells in embryos treated with either DMSO or inhibitors. Error bars indicate s.d. *$P<0.05$, **$P<0.01$, ***$P<0.001$ (unpaired, two-tailed *t*-test). All images are shown at the same magnification apart from the rightmost panel that exhibits a 2.5× increased magnification. Scale bars: 50 μm.

Nodal or Eph1 signalling inhibition, this result suggests that Nodal regulates the transition to step 2 at least in part through the transcriptional upregulation of *Eph1* in endoderm precursors. We cannot currently exclude that additional targets of Nodal are also involved.

Nodal-independent levels of Eph signalling are required to lengthen the cell cycle of endoderm precursors

We next analysed whether the Nodal-independent expression of *Eph1* in vegetal blastomeres may also have a function during gastrulation. Cytokinesis and interphase cell shape changes involve overlapping sets
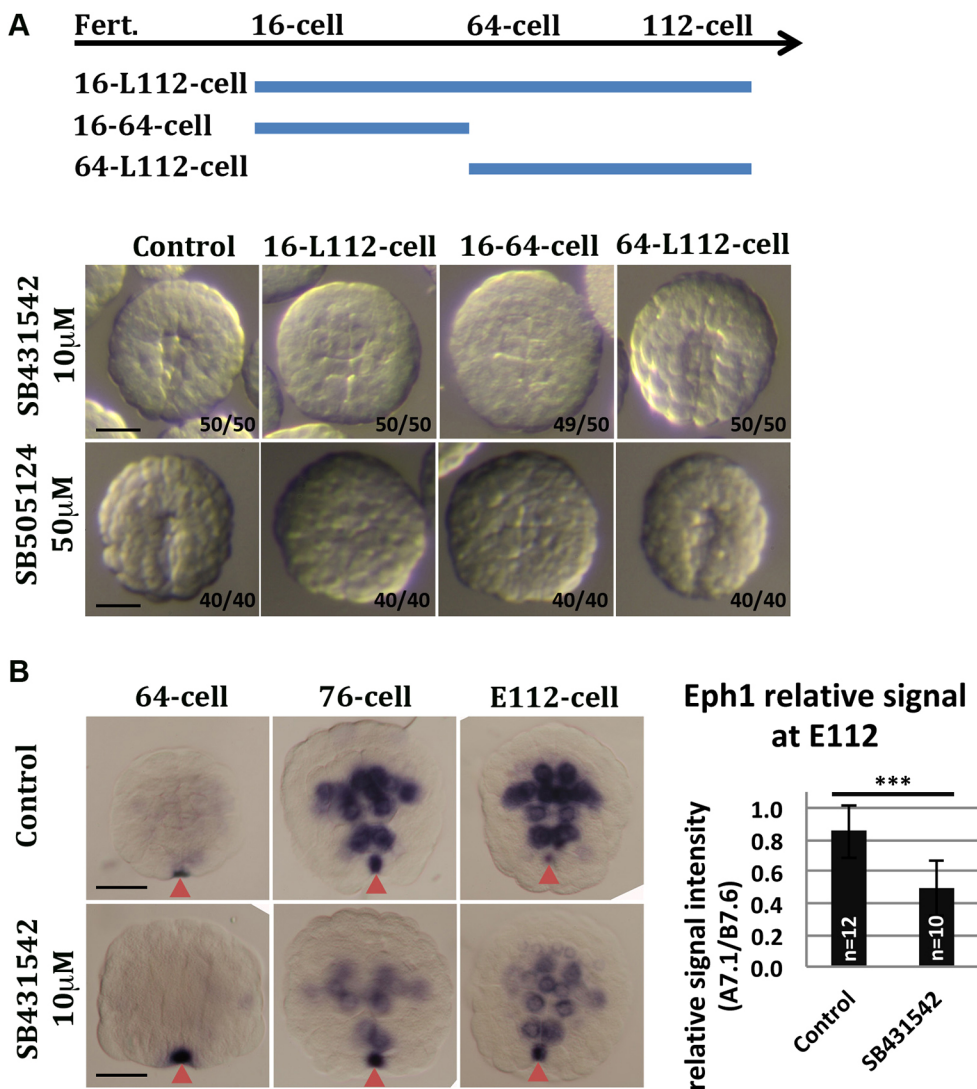
Fig. 5. Nodal signalling activity at the 32-cell stage regulates endoderm invagination and modulates *Eph1* expression in *P. mammillata*. (A) Temporal requirement of Nodal signals for endoderm invagination. *Phallusia* embryos were treated with two chemically-related competitive inhibitors of ATP binding in ALK4/5/7 SB431542 (10 µM) or SB505124 (50 µM) during different time windows as shown in the top schematic and analysed at the late 112-cell stage for invagination defects. The phenotype quantification is shown as the number of embryos exhibiting a phenotype/total number of embryos analysed. (B) *Eph1* WMISH at the 112-cell stage in control embryos and in embryos treated with 10 µM SB431542 from the 16-cell stage. Quantification of the relative *Eph1 in situ* signal at the 112-cell stage with: *Eph1* relative signal intensity=(mean A7.1 signal–mean background signal)/(mean B7.6 signal–mean background signal). ***$P<0.001$ (unpaired, two-tailed *t*-test). Error bars indicate s.d. Note that SB431542 treatment decreases zygotic *Eph1* expression without affecting its maternal expression in the presumptive germ cells (red arrowheads), which we used as an internal standard in the quantifications. Data representative of three independent experiments. Scale bars: 50 µm.

of cytoskeletal regulators (Duncan and Tin Su, 2004). Gastrulating cells therefore usually have a longer cell cycle than their neighbours, so as to postpone their mitosis until after completion of invagination. Indeed, endodermal precursors have a longer cell cycle than other vegetal cells (Nishida, 1987; Dumollard et al., 2013) and their division occurs after the completion of step 2 (Sherrard et al., 2010).

Full Nodal receptor inhibition or inhibition of Eph1 signalling with 6 µM NVPBHG712 from the 16-cell stage prevented step 2 without interfering with the timing of division of endoderm progenitors. By contrast, treatment of embryos with a higher concentration (8 µM) of NVPBHG712 led to a premature division of endoderm progenitors in 15.6% of *Phallusia*-treated embryos (Fig. 6A). Similarly, *Eph1* morpholino injection in *Ciona* led to the premature division of endoderm precursors (Fig. 6B).

We conclude that Eph1 has a dual role during endoderm invagination. Low Nodal-independent levels of *Eph1* expression are required to lengthen the cell cycle of endodermal precursors and postpone cell division until the completion of step 2. High Nodal-dependent levels of *Eph1* expression are then required for the transition between steps 1 and 2.

DISCUSSION
The invagination of endodermal progenitors at the onset of ascidian gastrulation involves a myosin-dependent two-step change of shape

of invaginating cells and a lengthening of their cell cycle. In this study, we identified two novel regulators of these processes: the Nodal TGF-β pathway and the Eph1 receptor tyrosine kinase pathway (Fig. 7). Both pathways are necessary for the transition between the two steps of cell shape changes and Nodal transcriptionally upregulates *Eph1*, suggesting that Eph1 signalling relays the information provided by Nodal. In addition, low Nodal-independent Eph1 signalling is required for the lengthening of the endodermal cell cycle. Our study also revealed that the inhibition of Nodal or Eph signalling, as well as that of ROCK, the major pathway controlling step 1, had no major effect on the fate of mesendodermal cells. Fate specification is thus in part uncoupled from the control of morphogenesis in early ascidian embryos.

An active transcriptional switch between apical constriction and apico-basal shortening
We previously showed that invagination involved a first step of apical constriction, driven by the activation of Myosin II by Rho kinase on the apical surface of endodermal progenitors, followed by a second step of apico-basal shortening driven by the Rho kinase-independent activation of Myosin II on the baso-lateral facets of invaginating cells (Sherrard et al., 2010). These two steps appear to be independent of one another, as inhibition of apical constriction does not affect apico-basal shortening (Sherrard et al., 2010).
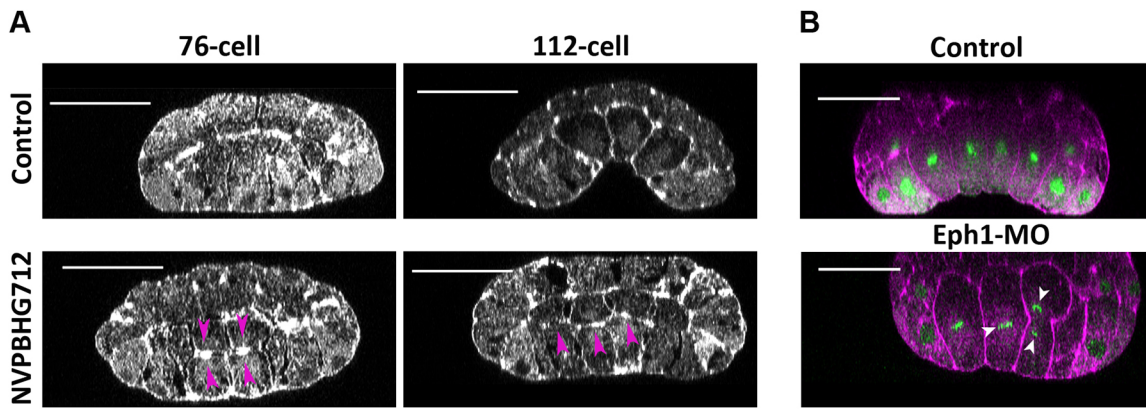
Fig. 6. Eph kinase inhibition and Eph1-MO microinjection induce premature endoderm cell division. (A) Frontal optical sections through 76- and late 112-cell stage *Phallusia* embryos treated with 8 μM NVPBHG712 from the 8-cell stage and stained for actin with phalloidin. Note the premature division of the endoderm progenitors (pink arrowheads); 10/64 (15.6%) analysed embryos treated with 8 μM NVPBHG712 from the 8-cell stage exhibited premature endoderm division, whereas none of the control embryos (*n*=81) showed this phenotype. (B) Frontal optical sections through early 112-cell *Ciona* embryos under control conditions or microinjected with Eph1-MO. Note the premature division of the endoderm progenitors (white arrowheads). The embryos are stained for actin with fluorescent phalloidin and for DNA with DAPI. Scale bars: 50 μm.

A similar situation is found during *Drosophila* gastrulation, as apical constriction can be blocked without affecting subsequent apico-basal shortening (Leptin, 1999). More generally, cells frequently switch from one behaviour to another during animal gastrulation (Davidson, 2012; Leptin, 2005). How the transitions between successive and independent modules are controlled at the molecular level remains mysterious. Such transition could involve direct mechanosensory feedbacks, transcriptional processes or both.

By searching for signalling pathways involved in ascidian endoderm invagination, we discovered that Eph signalling inhibition stalls invaginating cells in a state corresponding to the end of apical constriction (Fig. 4), without affecting cell differentiation. This finding carries three major conceptual messages. First, the possibility to stall cells in an end-of-step 1 state reveals the existence of a coordination mechanism for the transition between the two consecutive steps. Although apical accumulation of 1P-Myosin is not required for step 2 (Sherrard

et al., 2010), our results suggest that clearance of apical 1P-Myosin acts as a checkpoint for the onset of step 2. Second, this checkpoint only acts on morphogenesis, as mesendoderm differentiation continues in the absence of Nodal/Eph signalling. Finally, our results identify the transcriptional upregulation of *Eph1* as a key component of the termination of apical 1P-Myosin accumulation, possibly through the inhibition of RhoA as observed for EphA4 in early *Xenopus* embryos (Winning et al., 2002). Although we cannot rule out the existence of additional direct mechanosensory feedback mechanisms within the cell cortex, the results presented here argue that the transition between the two steps is controlled at the transcriptional level by developmental gene regulatory networks.

Eph1 controls endoderm cell cycle length independently of Nodal

As mitosis and myosin-driven cell shape changes during interphase use overlapping sets of cytoskeletal proteins, cell division cannot be
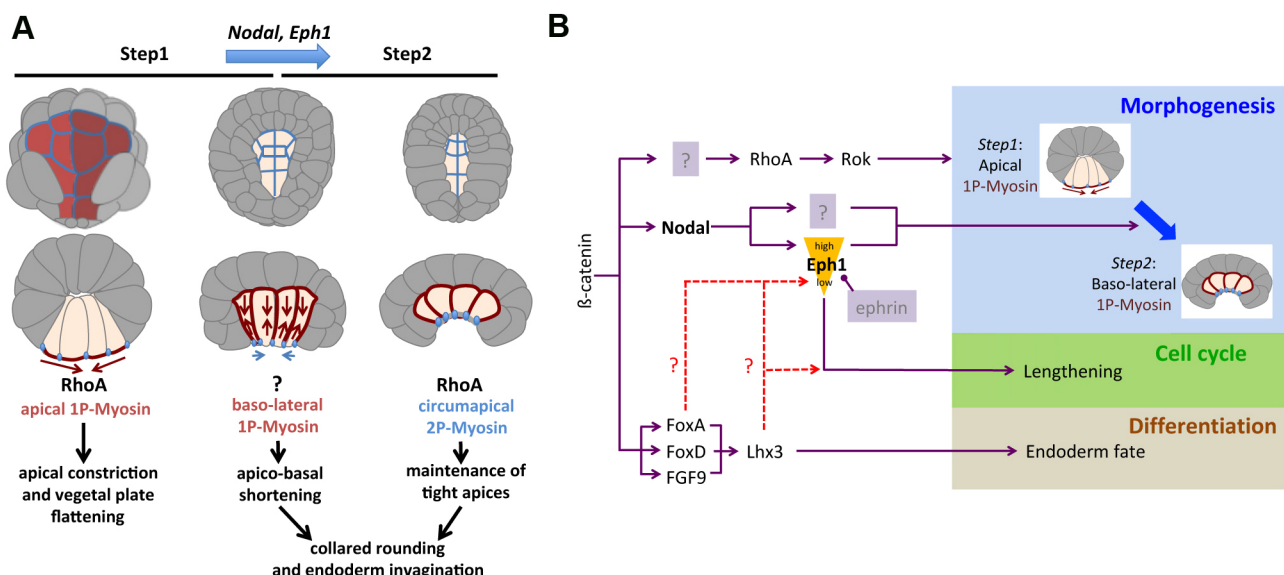

Fig. 7. Working model for the endoderm invagination regulatory network. (A) Regulatory mechanisms involved in endoderm cell shape changes during the 2-step process of ascidian endoderm invagination. (B) Transcriptional regulatory network driving endoderm invagination.

executed during the invagination of epithelial cells (Duncan and Tin Su, 2004). In pre-gastrula and early gastrula ascidian embryos, the mitosis of endodermal progenitors is thus delayed until the end of their invagination (Nishida, 1986; Sherrard et al., 2010; Guignard et al., 2020). This cell cycle lengthening is controlled downstream of β-catenin-mediated transcriptional activation (Dumollard et al., 2013). In this study, we observed that endoderm precursors entered mitosis precociously when Eph signals were blocked with a higher dose of NVPBHG712P in *Phallusia* or Eph1-MO in *Ciona*. This observation constitutes the first identification of a zygotic control mechanism of mitosis timing in ascidians.

In *Drosophila* and *Xenopus*, mitotic delay during gastrulation is achieved by blocking the CDC25-mediated dephosphorylation of CDK1 (Großhans and Wieschaus, 2000; Murakami et al., 2004; Seher and Leptin, 2000). Eph signalling has previously been implicated in both positive (Genander et al., 2009) and negative (del Valle et al., 2011) control of cell proliferation in mammals. *In vivo*, Eph receptor activation can phosphorylate the Src kinase (Jungas et al., 2016), which is a negative regulator of CDK1 (Horiuchi et al., 2018). *In vitro*, many Eph receptors can also directly phosphorylate CDK1 on its inhibitory regulatory Tyr15 residue (Blouin et al., 2011). Future studies will explore whether Eph1 delays mitosis of endodermal progenitors via the inhibition of CDK1 activity during ascidian gastrulation as well.

Evolution of the function of Nodal during chordate gastrulation

In vertebrates, Nodal connects embryonic patterning and morphogenesis. In *Xenopus*, zebrafish and mammals, it controls both the induction of mesendodermal fates and the control of gastrulation movements, through the activation of partially distinct sets of target genes (Arnold et al., 2008; Kikuchi et al., 2001; Popov et al., 2018; Woo et al., 2012; Yasuo and Lemaire, 1999). As a result, the cell autonomous activation of the Nodal receptor is sufficient in zebrafish to convert naïve ectodermal cells into ingressing endodermal precursors (Liu et al., 2018). Temporal analysis of Nodal signalling requirements in *Xenopus* and zebrafish indicated that this pathway has a pre-gastrula function in mesendoderm induction and subsequently controls gastrulation movements, independently of its fate specification function (Luxardi et al., 2010; Woo et al., 2012).

In ascidians, *Nodal* is broadly expressed in most vegetal cells at the 32-cell stage, including cells that will not invaginate. Although Nodal is dispensable for endoderm induction, its morphogenetic activity needs to be gated by fate specification cues to only affect endoderm precursors. Our work indicates that the spatial control of *Eph1* expression gates the action of Nodal. We found that two independent regulatory inputs control the expression profile of *Eph1*. Fate specification regulatory networks ensure that this gene is mostly expressed in endoderm precursors from the 64-cell stage, where it is required to delay mitosis. Nodal signals increase *Eph1* expression to a level sufficient to trigger the transition to step 2 of invagination (see summary in Fig. 7).

Vertebrates and ascidians thus use two different strategies to integrate fate specification and gastrulation. In vertebrates, Nodal controls both aspects, through the activation of distinct regulatory programs. In ascidians, Nodal controls invagination without acting on mesendoderm specification, but one of its targets, Eph1, integrates morphogenetic and fate information. Of note, Nodal controls neither endoderm induction nor gastrulation in *Amphioxus* or sea urchins, in which its role is restricted to axial patterning (Duboc and Lepage, 2008; Onai et al., 2010). It is thus tempting to propose that the gastrulation function of Nodal is a novelty of the olfactores, the grouping of tunicates and vertebrates.

Consistently, Nodal controls gastrulation movements in both vertebrates and ascidians by modulating actomyosin contractility of the cortex of mesendodermal cells (Krieg et al., 2008; Popov et al., 2018). Interestingly, in *Xenopus* Nodal signalling is necessary for normal EphA4 expression in the mesoderm (Wills and Baker, 2015) and both signalling pathways are required for the internalization of the mesendoderm (Evren et al., 2014). The presence of this association in both taxa is suggestive of an ancestral state. There may, however, also be differences in the mode of action of Nodal across olfactores. For example, although Nodal triggers apico-basal shortening through the termination of the Rho-dependent apical accumulation of 1P-Myosin at the end of ascidian apical constriction, this pathway triggers the apico-basal elongation of *Xenopus* bottle cells through activation of the *plekhg5* RhoGEF (Popov et al., 2018).

The identification and comparison of Nodal and Eph targets during early ascidian and vertebrate embryogenesis will help in assessing the respective share of ancestral and convergent mechanisms acting downstream of Nodal during gastrulation.

MATERIALS AND METHODS
Embryo culture conditions
Adult *P. mammillata* and *C. intestinalis* (formerly known as *C. intestinalis* type B) (Brunetti et al., 2015; Pennati et al., 2015) were collected on the Northern shore of Brittany by the marine facility of the Roscoff Marine Biological Station (France) and maintained in natural or artificial sea water at 16°C under constant illumination. Eggs were collected, fertilized and dechorionated as previously described (McDougall and Sardet, 1995; Robin et al., 2011).

Perturbation assays by chemical treatment
Phallusia embryos were treated with the MEK inhibitor U0126 (Calbiochem; 10 μM), the BMP signalling inhibitor Dorsomorphin (Sigma-Aldrich; 10 μM), the Nodal receptor inhibitors SB431542 (5 μM and 10 μM) and SB505124 (50 μM) (Sigma-Aldrich), the Eph inhibitor NVPBHG712 (Tocris Bioscience; 1, 2, 4, 6 or 8 μM) and with the Rho kinase inhibitor Y-27632 (Sigma-Aldrich; 100 μM) in artificial sea water at specific developmental stages as specified in the figures. *Ciona* embryos were treated with SB431542 and NVPBHG712 at 5 μM and 8 μM, respectively, at the developmental stages specified in the figures. The U0126, Dorsomorphin and SB431542/505124 inhibitor stocks were in DMSO. To compensate for a possible effect of the DMSO solvent, the control embryos in the various experiments were treated with the same concentration of DMSO as the experimental ones. Y-27632 was dissolved in water.

SB431542 and SB505124 are reported to be selective potent inhibitors for Alk4, Alk5 and Alk7 TGFβ receptors (DaCosta Byfield et al., 2004; Inman et al., 2002) and therefore inhibit the sole ascidian orthologue of these receptors. NVPBHG712 has been described as a highly selective small molecular weight inhibitor of Eph kinase activity (Martiny-Baron et al., 2010). SB431542, U0126, Dorsomorphin and Y27632 have previously been used in ascidian developmental studies (Hudson et al., 2003, 2007; Sherrard et al., 2010; Waki et al., 2015).

Gene identities
Gene identities for *Ciona* and *Phallusia* are listed in Table S1.

Microinjection of RNAs and morpholino oligonucleotides
Synthetic mRNA was produced using the mMESSAGE mMACHINE kit (Ambion) and microinjected as previously described (Hudson et al., 2003). Synthetic mRNA for the *Ciona* dominant negative Nodal receptor *Alk4/5/7* (Hudson and Yasuo, 2005) was microinjected at a concentration of 1.190 μg/μl. Morpholino-antisense oligonucleotides against *Ciinte Eph1*,

Eph1-MO (ATCTCCAATCTCCGGTCTGTTTGTC), were dissolved in water at a concentration of 0.7 mM before microinjection.

Whole-mount *in situ* hybridization

In situ hybridization experiments in *Phallusia* embryos were performed as previously described (Christiaen et al., 2009). Dig-labelled mRNA probes for *P. mammillata FoxA.a*, *Lhx3*, *Mycn*, *Perlecan* and *Ttf1* were synthesized from cDNA clones of the Villefranche-sur-mer *P. mammillata* cDNA clone collection (Brozovic et al., 2018) using the SP6/T7 DIG RNA labelling kit (Roche, 11175025910). Clones used for probe synthesis were: *FoxA.a*, AHC0AAA74YF05; *Lxh3*, AHC0AAA183YA13; *Mycn*, AHC0AAA60YB16; *Perlecan*, AHC0AAA215YL21; *Ttf1*, AHC0AAA267YK08.

Nodal (phmamm.g00015500), *Efna.c* (phmamm.g00000939) and *Eph1* (phmamm.g00004451) Dig-labelled mRNA probes were synthesized from cDNA produced from total mRNA (Superscript III Reverse transcriptase kit; Life Technologies) isolated from *Phallusia* at 32-cell stage for *Nodal* and at 112-cell stage for *Efna.c* and *Eph1* (RNeasy minikit; Qiagen). The primers introduce a T7 promoter (in bold) making the PCR product directly a probe synthesis template. The primers used to amplify the cDNA templates were: *Nodal*, forward 5′-CTATGGATATGACACAAGTATCGTTCTGC-3′ and reverse 5′-GATCC**TAATACGACTCACTATAGGG**TTATCGACAT-CCACATTCT-3′; *Eph1*, forward 5′-CCAACGTTGCGACTCCACTTTCA-CC-3′ and reverse 5′-ACGA**TAATACGACTCACTATAGGG**GTCTTG-GTTAGACATCTCCCAG-3′; *Efna.c*, forward 5′-CAACGAGGCATGTTC-TCTATTGGA-3′ and reverse 5′-GGATCC**TAATACGACTCACTATAG-**GATATGACGAAACCAGCAGTCAC-3′.

The protocols for *in situ* hybridization and alkaline phosphatase staining of *Ciona* embryos have been previously described (Hudson et al., 2013). Probes used include *Brachyury*, *Etr*, *Lhx3*, *Mrf*, *Ttf1* and *Twist-like-1* as previously described (Corbo et al., 1997; Hudson and Yasuo, 2006; Hudson et al., 2003, 2013; Meedel et al., 2007; Ristoratore et al., 1999).

Immunohistochemistry

Phalloidin-stained embryos were fixed in 4% formaldehyde in artificial sea water with HEPES (ASWH) at room temperature for 10 min, when not imaged in Murray's clear solution. Embryos imaged in Murray's clear solution were fixed in fixation solution [4% formaldehyde, 50 mM EGTA, 100 mM PIPES (pH 6.9), 400 mM sucrose] at room temperature for 10 min. After fixation the embryos were washed 3× in 0.1% Tween in PBS (PBT), 1× with PBS and stained with phalloidin (5 µl phalloidin per ml of PBS; Alexa Fluor546 phalloidin, A22283, Life Technologies) at 4°C overnight. The stained embryos were washed 3× with PBS and either mounted directly with mounting media (80% glycerol, 10% 10×PBS, 1.6% propyl gallate in H$_2$O) or dehydrated by going through an isopropanol series (70%, 85%, 95%, 100%, 100%) and then cleared by washing 3× in Murray's Clear solution (benzyl benzoate:benzyl alcohol; 2:1) and imaged in Murray's Clear solution.

Anti-phospho-myosin-stained embryos were fixed at room temperature for 30 min in fixation solution [100 mM HEPES (pH 7.0), 0.5 mM EGTA, 10 mM MgSO$_4$, 300 mM Dextrose, 0.2% Triton, 2% formaldehyde EM-grade, 0.2% glutaraldehyde]. Embryos were then washed 3× with PBT, 1× with PBS and quenched with 0.1% sodium borohydride in PBS for 20 min. They were blocked with 1% bovine serum albumin in PBT for 24 h and stained with primary antibody recognizing Ser19 phospho-myosin (1:50; rabbit, 3671S, Cell Signaling Technology) for 24 h. The samples were washed 3× in PBT and stained with a donkey anti-rabbit FITC or Alexa647 labelled secondary antibody (1:200; 711-095-152, Jackson ImmunoResearch or A21244, Molecular Probes), washed 3× with PBT and mounted in mounting media (Sherrard et al., 2010).

Imaging and image analysis

Phallusia confocal fluorescence imaging was performed with a Zeiss LSM780 using a 40× objective (NA 1.3), 1.2× zoom and a step of 1 µm between sections. Imaged embryos were oriented using Amira and cell dimensions measured with Fiji (Schindelin et al., 2012). Apical and basal area measurements in *Phallusia* correspond to the area along the last plane of

contact with lateral neighbour cells and not to the curved apical and basal surfaces.

In situ Eph1 relative signal intensities were determined on inverted *in situ* images using Fiji. The *in situ* images had the dimensions of 5185×3456 pixels. For the relative Eph1 signal intensity calculation the mean signal intensity in a constant area was measured in cells A7.1 (endoderm) and B7.6 (germ line) with a single measurement (area measured: 7556 pixels; circle of 98 pixels radius), as well as the mean background signal intensity with the average of three independent measurements per image (area measured: 485,200 pixels; circle of 786 pixels radius). The relative signal intensities were calculated using the formula: Eph1 relative signal intensity=(A7.1 mean signal−background signal)/(B7.6 mean signal−background mean signal).

1P-Myosin fluorescence signal quantification was performed on average projections of selected planes (projection of eight sections separated by 1 µm). The Fiji software was used to make measurements of fluorescence signal intensity. Two to three separate apical line measurements and four lateral line measurements were made to determine the average mean apical and lateral signal intensities. A constant area defined by an ellipse (20×5 µm) was used to measure the mean cytoplasmic signal. The relative apical and lateral signal intensities were determined as a ratio of the mean apical and lateral signals divided by the mean cytoplasmic signal.

Confocal imaging of *Ciona* embryos was carried out with a Leica SP5 using a 40× objective (NA 1.25), 1.5× zoom and a *z*-step of 1 µm. To measure apical surface areas and cell heights along the apico-basal axis of *Ciona* endoderm precursors, embryos were individually mounted and oriented so that the regions of interest face roughly to the objective. ImageJ (Schneider et al., 2012) was used to further orient acquired images and for measurements. For the *Ciona* images shown in Fig. S4C, fixed embryos were placed with their vegetal pole side up and photographed with a Leica Z16 APO with a Canon EOS 60D mounted on it.

Author contributions

Conceptualization: U.-M.F., T.N., H.Y., P.L.; Validation: U.-M.F., T.N., A.R., H.Y.; Formal analysis: U.-M.F., T.N., H.Y.; Investigation: U.-M.F., T.N., A.R., H.Y.; Resources: H.Y., P.L.; Writing - original draft: U.-M.F., H.Y., P.L.; Supervision: H.Y., P.L.; Project administration: H.Y., P.L.; Funding acquisition: H.Y., P.L.

Supplementary information

Supplementary information available online at
https://dev.biologists.org/lookup/doi/10.1242/dev.186965.supplemental

References

Arnold, S. J., Hofmann, U. K., Bikoff, E. K. and Robertson, E. J. (2008). Pivotal roles for eomesodermin during axis formation, epithelium-to-mesenchyme transition and endoderm specification in the mouse. *Development* **135**, 501-511. doi:10.1242/dev.014357

Blouin, J., Roby, P., Arcand, M., Beaudet, L. and Lipari, F. (2011). Catalytic specificity of human protein tyrosine kinases revealed by peptide substrate profiling. *Curr. Chem. Genomics* **5**, 115-121. doi:10.2174/1875397301105010115

Brozovic, M., Dantec, C., Dardaillon, J., Dauga, D., Faure, E., Gineste, M., Louis, A., Naville, M., Nitta, K. R., Piette, J. et al. (2018). ANISEED 2017: extending the integrated ascidian database to the exploration and evolutionary comparison of genome-scale datasets. *Nucleic Acids Res.* **46**, D718-D725. doi:10.1093/nar/gkx1108

Brunetti, R., Gissi, C., Pennati, R., Caicci, F., Gasparini, F. and Manni, L. (2015). Morphological evidence that the molecularly determined Ciona intestinalis type A and type B are different species: Ciona robusta and Ciona intestinalis. *J. Zool. Syst. Evol. Res.* **53**, 186-193. doi:10.1111/jzs.12101

Christiaen, L., Wagner, E., Shi, W. and Levine, M. (2009). Whole-mount in situ hybridization on sea squirt (Ciona intestinalis) embryos. *Cold Spring Harb. Protoc.* **2009**, pdb.prot5348. doi:10.1101/pdb.prot5348

Ciruna, B. and Rossant, J. (2001). FGF signaling regulates mesoderm cell fate specification and morphogenetic movement at the primitive streak. *Dev. Cell* **1**, 37-49. doi:10.1016/S1534-5807(01)00017-X

Corbo, J. C., Levine, M. and Zeller, R. W. (1997). Characterization of a notochord-specific enhancer from the Brachyury promoter region of the ascidian, Ciona intestinalis. *Development* **124**, 589-602.

Costa, M., Wilson, E. T. and Wieschaus, E. (1994). A putative cell signal encoded by the folded gastrulation gene coordinates cell shape changes during Drosophila gastrulation. *Cell* **76**, 1075-1089. doi:10.1016/0092-8674(94)90384-0

DaCosta Byfield, S., Major, C., Laping, N. J. and Roberts, A. B. (2004). SB-505124 is a selective inhibitor of transforming growth factor-β type I receptors ALK4, ALK5, and ALK7. *Mol. Pharmacol.* **65**, 744-752. doi:10.1124/mol.65.3.744

Darras, S. and Nishida, H. (2001). The BMP/CHORDIN antagonism controls sensory pigment cell specification and differentiation in the ascidian embryo. *Dev. Biol.* **236**, 271-288. doi:10.1006/dbio.2001.0339

Davidson, L. A. (2012). Epithelial machines that shape the embryo. *Trends Cell Biol.* **22**, 82-87. doi:10.1016/j.tcb.2011.10.005

del Valle, K., Theus, M. H., Bethea, J. R., Liebl, D. J. and Ricard, J. (2011). Neural progenitors proliferation is inhibited by EphB3 in the developing subventricular zone. *Int. J. Dev. Neurosci.* **29**, 9-14. doi:10.1016/j.ijdevneu.2010.10.005

Delsuc, F., Brinkmann, H., Chourrout, D. and Philippe, H. (2006). Tunicates and not cephalochordates are the closest living relatives of vertebrates. *Nature* **439**, 965-968. doi:10.1038/nature04336

Delsuc, F., Philippe, H., Tsagkogeorga, G., Simion, P., Tilak, M.-K., Turon, X., López-Legentil, S., Piette, J., Lemaire, P. and Douzery, E. J. P. (2018). A phylogenomic framework and timescale for comparative studies of tunicates. *BMC Biol.* **16**, 39. doi:10.1186/s12915-018-0499-2

Duboc, V. and Lepage, T. (2008). A conserved role for the nodal signaling pathway in the establishment of dorso-ventral and left–right axes in deuterostomes. *J. Exp. Zool. B Mol. Dev. Evol.* **310B**, 41-53. doi:10.1002/jez.b.21121

Dumollard, R., Hebras, C., Besnardeau, L. and McDougall, A. (2013). Beta-catenin patterns the cell cycle during maternal-to-zygotic transition in urochordate embryos. *Dev. Biol.* **384**, 331-342. doi:10.1016/j.ydbio.2013.10.007

Duncan, T. and Tin Su, T. (2004). Embryogenesis: coordinating cell division with gastrulation. *Curr. Biol.* **14**, R305-R307. doi:10.1016/j.cub.2004.03.050

Evren, S., Wen, J. W. H., Luu, O., Damm, E. W., Nagel, M. and Winklbauer, R. (2014). EphA4-dependent Brachyury expression is required for dorsal mesoderm involution in the Xenopus gastrula. *Development* **141**, 3649-3661. doi:10.1242/dev.111880

Genander, M., Halford, M. M., Xu, N.-J., Eriksson, M., Yu, Z., Qiu, Z., Martling, A., Greicius, G., Thakar, S., Catchpole, T. et al. (2009). Dissociation of EphB2 signaling pathways mediating progenitor cell proliferation and tumor suppression. *Cell* **139**, 679-692. doi:10.1016/j.cell.2009.08.048

Großhans, J. and Wieschaus, E. (2000). A genetic link between morphogenesis and cell division during formation of the ventral furrow in Drosophila. *Cell* **101**, 523-531. doi:10.1016/S0092-8674(00)80862-4

Guignard, L., Fiuza, U.-M., Leggio, B., Laussu, J., Faure, E., Michelin, G., Biasuz, K., Hufnagel, L., Malandain, G., Godin, C. and Lemaire, P. (2020). Contact area-dependent cell communication and the morphological invariance of ascidian embryogenesis. *Science* **369**, eaar5663. doi:10.1126/science.aar5663

Heisenberg, C.-P. and Solnica-Krezel, L. (2008). Back and forth between cell fate specification and movement during vertebrate gastrulation. *Curr. Opin. Genet. Dev.* **18**, 311-316. doi:10.1016/j.gde.2008.07.011

Horiuchi, M., Kuga, T., Saito, Y., Nagano, M., Adachi, J., Tomonaga, T., Yamaguchi, N. and Nakayama, Y. (2018). The tyrosine kinase v-Src causes mitotic slippage by phosphorylating an inhibitory tyrosine residue of Cdk1. *J. Biol. Chem.* **293**, 15524-15537. doi:10.1074/jbc.RA118.002784

Hudson, C. and Yasuo, H. (2005). Patterning across the ascidian neural plate by lateral nodal signalling sources. *Development* **132**, 1199-1210. doi:10.1242/dev.01688

Hudson, C. and Yasuo, H. (2006). A signalling relay involving nodal and delta ligands acts during secondary notochord induction in Ciona embryos. *Development* **133**, 2855-2864. doi:10.1242/dev.02466

Hudson, C., Darras, S., Caillol, D., Yasuo, H. and Lemaire, P. (2003). A conserved role for the MEK signalling pathway in neural tissue specification and posteriorisation in the invertebrate chordate, the ascidian Ciona intestinalis. *Development* **130**, 147-159. doi:10.1242/dev.00200

Hudson, C., Lotito, S. and Yasuo, H. (2007). Sequential and combinatorial inputs from nodal, Delta2/notch and FGF/MEK/ERK signalling pathways establish a grid-like organisation of distinct cell identities in the ascidian neural plate. *Development* **134**, 3527-3537. doi:10.1242/dev.002352

Hudson, C., Kawai, N., Negishi, T. and Yasuo, H. (2013). β-catenin-driven binary fate specification segregates germ layers in ascidian embryos. *Curr. Biol.* **23**, 491-495. doi:10.1016/j.cub.2013.02.005

Imai, K., Takada, N., Satoh, N. and Satou, Y. (2000). (beta)-catenin mediates the specification of endoderm cells in ascidian embryos. *Development* **127**, 3009-3020.

Imai, K. S., Hino, K., Yagi, K., Satoh, N. and Satou, Y. (2004). Gene expression profiles of transcription factors and signaling molecules in the ascidian embryo: towards a comprehensive understanding of gene networks. *Development* **131**, 4047-4058. doi:10.1242/dev.01270

Imai, K. S., Levine, M., Satoh, N. and Satou, Y. (2006). Regulatory blueprint for a chordate embryo. *Science* **312**, 1183-1187. doi:10.1126/science.1123404

Inman, G. J., Nicolás, F. J., Callahan, J. F., Harling, J. D., Gaster, L. M., Reith, A. D., Laping, N. J. and Hill, C. S. (2002). SB-431542 is a potent and specific inhibitor of transforming growth factor-β superfamily type I activin receptor-like kinase (ALK) receptors ALK4, ALK5, and ALK7. *Mol. Pharmacol.* **62**, 65-74. doi:10.1124/mol.62.1.65

Jiang, D., Munro, E. M. and Smith, W. C. (2005). Ascidian prickle regulates both mediolateral and anterior-posterior cell polarity of notochord cells. *Curr. Biol.* **15**, 79-85. doi:10.1016/j.cub.2004.12.041

Jungas, T., Perchey, R. T., Fawal, M., Callot, C., Froment, C., Burlet-Schiltz, O., Besson, A. and Davy, A. (2016). Eph-mediated tyrosine phosphorylation of citron kinase controls abscission. *J. Cell Biol.* **214**, 555-569. doi:10.1083/jcb.201602057

Kiecker, C., Bates, T. and Bell, E. (2016). Molecular specification of germ layers in vertebrate embryos. *Cell. Mol. Life Sci.* **73**, 923-947. doi:10.1007/s00018-015-2092-y

Kikuchi, Y., Agathon, A., Alexander, J., Thisse, C., Waldron, S., Yelon, D., Thisse, B. and Stainier, D. Y. R. (2001). casanova encodes a novel Sox-related protein necessary and sufficient for early endoderm formation in zebrafish. *Genes Dev.* **15**, 1493-1505. doi:10.1101/gad.892301

Krieg, M., Arboleda-Estudillo, Y., Puech, P.-H., Käfer, J., Graner, F., Müller, D. J. and Heisenberg, C.-P. (2008). Tensile forces govern germ-layer organization in zebrafish. *Nat. Cell Biol.* **10**, 429-436. doi:10.1038/ncb1705

Krupke, O. A. and Burke, R. D. (2014). Eph-Ephrin signaling and focal adhesion kinase regulate actomyosin-dependent apical constriction of ciliary band cells. *Development* **141**, 1075-1084. doi:10.1242/dev.100123

Lee, J.-Y., Marston, D. J., Walston, T., Hardin, J., Halberstadt, A. and Goldstein, B. (2006). Wnt/Frizzled signaling controls C. elegans gastrulation by activating actomyosin contractility. *Curr. Biol.* **16**, 1986-1997. doi:10.1016/j.cub.2006.08.090

Lemaire, P. (2011). Evolutionary crossroads in developmental biology: the tunicates. *Development* **138**, 2143-2152. doi:10.1242/dev.048975

Leptin, M. (1999). Gastrulation in Drosophila: the logic and the cellular mechanisms. *EMBO J.* **18**, 3187-3192. doi:10.1093/emboj/18.12.3187

Leptin, M. (2005). Gastrulation movements: the logic and the nuts and bolts. *Dev. Cell* **8**, 305-320. doi:10.1016/j.devcel.2005.02.007

Liu, Z., Woo, S. and Weiner, O. D. (2018). Nodal signaling has dual roles in fate specification and directed migration during germ layer segregation in zebrafish. *Development* **145**, dev163535. doi:10.1242/dev.163535

Luxardi, G., Marchal, L., Thomé, V. and Kodjabachian, L. (2010). Distinct Xenopus nodal ligands sequentially induce mesendoderm and control gastrulation movements in parallel to the Wnt/PCP pathway. *Development* **137**, 417-426. doi:10.1242/dev.039735

Madgwick, A., Magri, M. S., Dantec, C., Gailly, D., Fiuza, U.-M., Guignard, L., Hettinger, S., Gomez-Skarmeta, J. L. and Lemaire, P. (2019). Evolution of embryonic cis-regulatory landscapes between divergent Phallusia and Ciona ascidians. *Dev. Biol.* **448**, 71-87. doi:10.1016/j.ydbio.2019.01.003

Martiny-Baron, G., Holzer, P., Billy, E., Schnell, C., Brueggen, J., Ferretti, M., Schmiedeberg, N., Wood, J. M., Furet, P. and Imbach, P. (2010). The small molecule specific EphB4 kinase inhibitor NVP-BHG712 inhibits VEGF driven angiogenesis. *Angiogenesis* **13**, 259-267. doi:10.1007/s10456-010-9183-z

McDougall, A. and Sardet, C. (1995). Function and characteristics of repetitive calcium waves associated with meiosis. *Curr. Biol.* **5**, 318-328. doi:10.1016/S0960-9822(95)00062-5

Meedel, T. H., Chang, P. and Yasuo, H. (2007). Muscle development in Ciona intestinalis requires the b-HLH myogenic regulatory factor gene Ci-MRF. *Dev. Biol.* **302**, 333-344. doi:10.1016/j.ydbio.2006.09.043

Murakami, M. S., Moody, S. A., Daar, I. O. and Morrison, D. K. (2004). Morphogenesis during Xenopus gastrulation requires Wee1-mediated inhibition of cell proliferation. *Development* **131**, 571-580. doi:10.1242/dev.00971

Nishida, H. (1986). Cell Division pattern during gastrulation of the ascidian, Halocynthia roretzi. *Dev. Growth Differ.* **28**, 191-201. doi:10.1111/j.1440-169X.1986.00191.x

Nishida, H. (1987). Cell lineage analysis in ascidian embryos by intracellular injection of a tracer enzyme: III. Up to the tissue restricted stage. *Dev. Biol.* **121**, 526-541. doi:10.1016/0012-1606(87)90188-6

Ohta, N. and Satou, Y. (2013). Multiple signaling pathways coordinate to induce a threshold response in a chordate embryo. *PLoS Genet.* **9**, e1003818. doi:10.1371/journal.pgen.1003818

Onai, T., Yu, J.-K., Blitz, I. L., Cho, K. W. Y. and Holland, L. Z. (2010). Opposing nodal/Vg1 and BMP signals mediate axial patterning in embryos of the basal chordate amphioxus. *Dev. Biol.* **344**, 377-389. doi:10.1016/j.ydbio.2010.05.016

Pennati, R., Ficetola, G. F., Brunetti, R., Caicci, F., Gasparini, F., Griggio, F., Sato, A., Stach, T., Kaul-Strehlow, S., Gissi, C. et al. (2015). Morphological differences between larvae of the Ciona intestinalis species complex: hints for a valid taxonomic definition of distinct species. *PLoS ONE* **10**, e0122879. doi:10.1371/journal.pone.0122879

Picco, V., Hudson, C. and Yasuo, H. (2007). Ephrin-Eph signalling drives the asymmetric division of notochord/neural precursors in Ciona embryos. *Development* **134**, 1491-1497. doi:10.1242/dev.003939

Popov, I. K., Ray, H. J., Skoglund, P., Keller, R. and Chang, C. (2018). The RhoGEF protein Plekhg5 regulates apical constriction of bottle cells during gastrulation. *Development* **145**, dev168922. doi:10.1242/dev.168922

Ristoratore, F., Spagnuolo, A., Aniello, F., Branno, M., Fabbrini, F. and Lauro, R. D. (1999). Expression and functional analysis of Cititf1, an ascidian NK-2 class gene, suggest its role in endoderm development. *Development* **126**, 5149-5159.

Robin, F. B., Dauga, D., Tassy, O., Sobral, D., Daian, F. and Lemaire, P. (2011). Time-lapse imaging of live phallusia embryos for creating 3D digital replicas. *Cold Spring Harb. Protoc.* **2011**, 1244-1246. doi:10.1101/pdb.prot065847

Schindelin, J., Arganda-Carreras, I., Frise, E., Kaynig, V., Longair, M., Pietzsch, T., Preibisch, S., Rueden, C., Saalfeld, S., Schmid, B. et al. (2012). Fiji: an open-source platform for biological-image analysis. *Nat. Methods* **9**, 676-682. doi:10.1038/nmeth.2019

Schneider, C. A., Rasband, W. S. and Eliceiri, K. W. (2012). NIH image to imageJ: 25 years of image analysis. *Nat. Methods* **9**, 671-675. doi:10.1038/nmeth.2089

Seher, T. C. and Leptin, M. (2000). Tribbles, a cell-cycle brake that coordinates proliferation and morphogenesis during Drosophila gastrulation. *Curr. Biol.* **10**, 623-629. doi:10.1016/S0960-9822(00)00502-9

Sherrard, K., Robin, F., Lemaire, P. and Munro, E. (2010). Sequential activation of apical and basolateral contractility drives ascidian endoderm invagination. *Curr. Biol.* **20**, 1499-1510. doi:10.1016/j.cub.2010.06.075

Shi, W. and Levine, M. (2008). Ephrin signaling establishes asymmetric cell fates in an endomesoderm lineage of the Ciona embryo. *Development* **135**, 931-940. doi:10.1242/dev.011940

Solnica-Krezel, L. and Sepich, D. S. (2012). Gastrulation: making and shaping germ layers. *Annu. Rev. Cell Dev. Biol.* **28**, 687-717. doi:10.1146/annurev-cellbio-092910-154043

Von der Hardt, S., Bakkers, J., Inbal, A., Carvalho, L., Solnica-Krezel, L., Heisenberg, C.-P. and Hammerschmidt, M. (2007). The Bmp gradient of the zebrafish gastrula guides migrating lateral cells by regulating cell-cell adhesion. *Curr. Biol.* **17**, 475-487. doi:10.1016/j.cub.2007.02.013

Waki, K., Imai, K. S. and Satou, Y. (2015). Genetic pathways for differentiation of the peripheral nervous system in ascidians. *Nat. Commun.* **6**, 8719. doi:10.1038/ncomms9719

Wills, A. E. and Baker, J. C. (2015). E2a is necessary for Smad2/3-dependent transcription and the direct repression of lefty during gastrulation. *Dev. Cell* **32**, 345-357. doi:10.1016/j.devcel.2014.11.034

Winning, R. S., Ward, E. K., Scales, J. B. and Walker, G. K. (2002). EphA4 catalytic activity causes inhibition of RhoA GTPase in Xenopus laevis embryos. *Differentiation* **70**, 46-55. doi:10.1046/j.1432-0436.2002.700105.x

Woo, S., Housley, M. P., Weiner, O. D. and Stainier, D. Y. R. (2012). Nodal signaling regulates endodermal cell motility and actin dynamics via Rac1 and Prex1. *J. Cell Biol.* **198**, 941-952. doi:10.1083/jcb.201203012

Yasuo, H. and Hudson, C. (2007). FGF8/17/18 functions together with FGF9/16/20 during formation of the notochord in Ciona embryos. *Dev. Biol.* **302**, 92-103. doi:10.1016/j.ydbio.2006.08.075

Yasuo, H. and Lemaire, P. (1999). A two-step model for the fate determination of presumptive endodermal blastomeres in Xenopus embryos. *Curr. Biol.* **9**, 869-879. doi:10.1016/S0960-9822(99)80391-1

Yu, P. B., Hong, C. C., Sachidanandan, C., Babitt, J. L., Deng, D. Y., Hoyng, S. A., Lin, H. Y., Bloch, K. D. and Peterson, R. T. (2008). Dorsomorphin inhibits BMP signals required for embryogenesis and iron metabolism. *Nat. Chem. Biol.* **4**, 33-41. doi:10.1038/nchembio.2007.54